

# Solidification of Simulated $\alpha$ -HLLW in Iron Phosphate Glass-Ceramics

Pan Sheqi, Wan Xiaogang, Xi Chengcheng, Su Wei, Zhang Hailing and Wang Yongpeng

**Abstract** Using iron boron phosphate glass to immobilize simulated  $\alpha$ -HLLW has been studied. The results showed that sintering at a temperature of 930 °C, heating for 2 h, monazite-type crystal was detected only by XRD apparatus in the solidification. The samples containing different contents of simulated  $\alpha$ -HLLW were measured by product consistency test (PCT) and showed the maximum pack capacity of up to 25% with a good chemical durability, and the normalized elemental mass release of Fe, P, and Ce is  $28.10 \times 10^{-4} \text{g}\cdot\text{m}^{-2}\cdot\text{d}^{-1}$ ,  $56.61 \times 10^{-4} \text{g}\cdot\text{m}^{-2}\cdot\text{d}^{-1}$ , and  $0.95 \times 10^{-4} \text{g}\cdot\text{m}^{-2}\cdot\text{d}^{-1}$ , respectively.

**Keywords**  $\alpha$ -HLLW · Iron phosphate glass · Solidification

## 1 Introduction

The spent fuel reprocessing will generate large quantities of high-level nuclear wastes, which need to be vitrified before deep geological disposal. Deep geological disposal is an appropriate method for the high-level radioactive waste disposal, whose purpose is to further isolate the waste from the biosphere system. In order to minimize the environmental impact of spent fuel discharged from nuclear power

---

P. Sheqi · W. Xiaogang · X. Chengcheng · S. Wei · Z. Hailing · W. Yongpeng (✉)  
Institute of Materials, China Academy of Engineering Physics, Mianyang, China  
e-mail: wangyongpeng@caep.cn

P. Sheqi  
e-mail: pansheqi@caep.cn

W. Xiaogang  
e-mail: wanxiaogan@caep.cn

X. Chengcheng  
e-mail: xichengcheng@caep.cn

S. Wei  
e-mail: suwei@caep.cn

reactors and the final volume of solidification matrix in the repository, TRPO (trialkyl phosphine oxide) extraction process was developed. With TRPO method, minor actinides and long-lived fission products containing little Sr and Cs can be separated from wastes and then be vitrified, making the radioactivity of original wastewater greatly decreased. Former high-level liquid wastes turn to be of low-intermediate level and short-lived wastes, which can be solidified by cement for future surface disposal. Borosilicate glass is widely used for vitrification of high-level nuclear wastes. However, borosilicate glasses are not a good option for vitrification of sulfate- or phosphate-bearing wastes as the problem of “yellow phase” often appeared in the vitrification melter, when sulfate or phosphate was present. Hence, waste loading of such glasses had to be lowered sharply, resulting in poor economy [1–4]. Meanwhile, iron phosphate glass is considered as a practical alternative for vitrifying such nuclear wastes not well suited for borosilicate glass due to its excellent resistance to water erosion, low viscosity under high-temperature melting conditions, and relatively low handling temperature. Iron phosphate glass has caught extensive attention since it was reported by Sales et al. in 1984. The chemical and thermal durability of iron phosphate glass would be both enhanced to some extent when appropriate amount of  $B_2O_3$  was doped. In addition, the thermal neutron absorption coefficient for  $B_2O_3$  was about two orders of magnitude higher than  $P_2O_5$ . All these factors make iron phosphate glass more suitable to immobilize such high-level radioactive waste.

In this study, the iron phosphate glass vitrification technology for the main components of  $\alpha$ -waste derived from TRPO extraction procedure was investigated, which would provide necessary fundamental data and technical support for the widespread application of such vitrification technology in practice.

## 1.1 Materials and Methods

### 1.1.1 Formula Design of Simulated High-Level Radioactive Waste

The main components of TRPO extracts can be seen in Table 1, which contains almost all actinide elements. Considering material source and safety during test, simulated high-level radioactive waste used did not contain neodymium, uranium, and transuranium elements, which were replaced by equal stoichiometric amount of cerium. According to the data listed in Table 1, the oxide contents of each element were also calculated stoichiometrically, and their respective mass fractions in our simulated high-level radioactive waste are listed in Table 2. The carefully weighed oxides were first stirred and powdered using ball mill and then dried before use.

**Table 1** Main components of TRPO extracts

| Components    | Fe   | La     | Ce     | Nd    | Mo  | Zr   | TRU+U |
|---------------|------|--------|--------|-------|-----|------|-------|
| Content (g/l) | 0.34 | 0.5865 | 0.7755 | 2.038 | 0.5 | 0.01 | 1.83  |

**Table 2** Oxide contents of each element in simulated high-level radioactive waste

| Oxidation   | Fe <sub>2</sub> O <sub>3</sub> | La <sub>2</sub> O <sub>3</sub> | CeO <sub>2</sub> | MoO <sub>3</sub> | ZrO <sub>2</sub> |
|-------------|--------------------------------|--------------------------------|------------------|------------------|------------------|
| Content/wt% | 7.40                           | 33.94                          | 47.02            | 11.43            | 0.21             |

### 1.1.2 Specimen Preparation and Sintering

Simulated high-level radioactive waste and basic glass were firstly adequately blended at a proper ratio in mortars, then were pressed to form briquettes at 20 MPa with 5% polyvinyl alcohol (PVA) added as binders. The rough briquettes were powdered and sifted through 140-mesh sieve after drying for 24 h at 110 °C. Mixed with a certain amount of binders, the powdered briquettes were again pressed at 30 MPa to form specimen. Program temperature rise is used for specimen sintering. First temperature was raised at the rate of 1 °C/min until 500 °C, then kept at 500 °C for 5 h to remove the binders, then raised again at 3 °C/min until the required temperature and kept warm for certain time. Finally, the specimen was naturally cooled to room temperature.

### 1.1.3 Analytical Measurements and Calculations

The crystalline phase of samples was examined with X-ray diffraction (XRD) (Rigaku D/max IIIA Co., Japan) with Cu K $\alpha$ 1 radiation. Sample density ( $\rho$ , g/cm<sup>3</sup>) was measured using Archimedes method at 25 °C with distilled water as liquid medium. The chemical durability of samples were determined by the product consistency test (PCT, ASTM C-1285-02), procedures of which were as follows: Particles screened through mesh size of 100–200 (diameter, 75–150  $\mu$ m) were firstly washed several times with ethanol and deionized water under ultrasonic conditions and then dried according to the standard. About 3.0 g precisely weighted particles and 30 mL deionized water were placed in polythene bottles and dried in ovens with temperature controlled at 90  $\pm$  2 °C. Each element's mass concentration in the liquid after 7 days of erosion was measured using ultraviolet-visible spectrophotometry, and the normalized element mass release (LR<sub>*j*</sub>, g m<sup>-2</sup> d<sup>-1</sup>) was calculated according to the equation below:

$$LR_j = c_j/w_j \cdot (A_s/V) \cdot t$$

In the equation,  $c_j$  stands for the mass concentration of element  $j$  (mg L<sup>-1</sup> or g m<sup>-3</sup>);  $w_j$ , which was calculated based on the composition of the glass, stands for elemental mass fraction in the sample;  $A_s/V$  stands for the ratio between total surface of solid particles ( $A_s$ ) and volume of erosion liquid ( $V$ ), which was taken as 2000 m<sup>-1</sup> in consistence with PCT standard, while  $t$  stands for erosion time (d).

## 1.2 Results and Discussion

### 1.2.1 Sintering Temperature

XRD spectrograms of simulated radioactive waste with 20% waste loading obtained at different sintering temperatures were shown in Fig. 1. As shown, principal crystalline phase of monazite was detected in all solidification matrixes sintered over a relatively wide temperature range, indicating that the elements in simulated waste, like Ce, La, could exist steadily in the glass in the form of monazite, making such glass own a much better waste-holding stability than normal borosilicate glass [5].

When sintering temperature was raised from 800 to 950 °C, the XRD patterns of monazite in the solidification became clearer, with sharper peaks and fewer diffuse peaks. However, when sintering temperature was raised again over 1000 °C, part peaks for monazite appeared diffuse, revealing a decrease in specimen's crystallinity. With the further rise in sintering temperature, the growth and movement of crystals became faster. The initial crystals grew up quickly and blocked their adjacent crystals' growth, and the crystal–glass interface number was reduced, which would be unbeneficial for the formation of crystallite structure and cause structural defects in crystallite. Specimen's crystallinity under different sintering temperatures was calculated using MDI Jade 5.0 (Table 3). Hence, iron boron phosphate–monazite-type glass-ceramic solidified body should be sintered at 900–950 °C, according to XRD analysis and crystallinity calculation results.

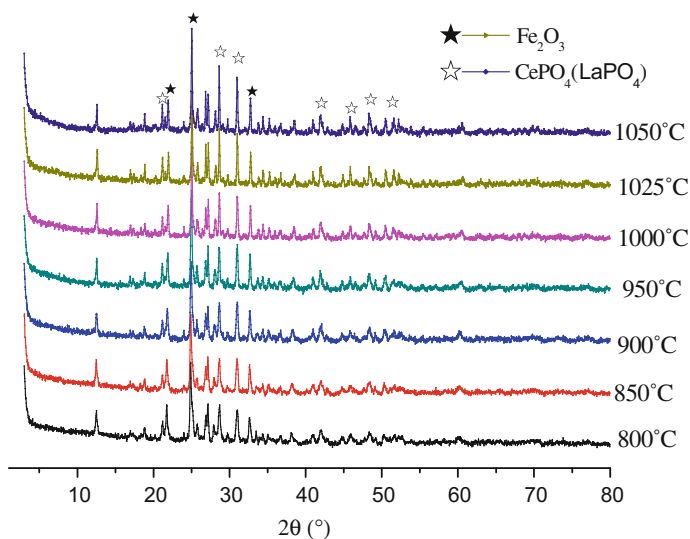


**Fig. 1** XRD spectrograms of simulated radioactive waste with 20% waste loading obtained at different sintering temperatures

**Table 3** Specimen's crystallinity under different sintering temperatures

| Sintering temperature (°C) | 800   | 850   | 900   | 950   | 1000  | 1025  | 1050  |
|----------------------------|-------|-------|-------|-------|-------|-------|-------|
| Crystallinity (%)          | 80.66 | 78.87 | 85.47 | 86.72 | 82.37 | 82.36 | 79.39 |

### 1.2.2 Holding Time

Holding time is another important parameter for sintering process. Prolonging holding time at certain sintering temperature would promote the growth of crystalline grains in component-fixed glass-ceramic. The crystalline grains would be more uniform in size, and overall structure and performance would be improved of the glass-ceramic. Figure 2 shows the XRD patterns of specimens produced at equal sintering temperature (950 °C) but different holding time, while the corresponding crystallinity results were listed in Table 4. The XRD patterns for monazite in each specimen in Fig. 2 were nearly the same, which was consistent with the crystallinity results. Hence, the holding time for specimen should be 1–2 h under such sintering condition since prolonging holding time would not bring better performance to glass-ceramic. In addition, prolonging holding time increased the occurrence of abnormal grain growth, which was also not economically feasible.

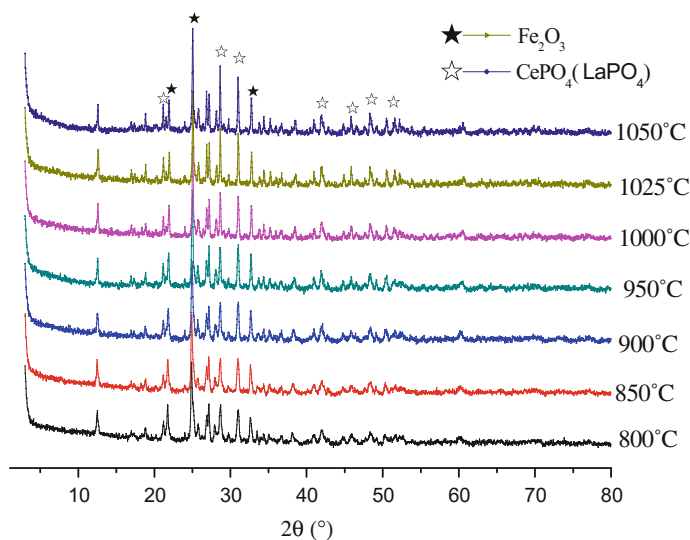


**Fig. 2** XRD patterns of specimens produced at equal sintering temperature (950 °C) but different holding time

**Table 4** Crystallinity results at different holding time

| Holding time (h)  | 1     | 2     | 3     | 4     | 5     |
|-------------------|-------|-------|-------|-------|-------|
| Crystallinity (%) | 84.69 | 86.17 | 86.64 | 85.18 | 84.10 |

### 1.2.3 Parameter Optimization for Densification Process

Glass-ceramic solidification of high-level radioactive waste slurry was to make the vast majority of actinide elements enter into the lattice of ceramics, forming solid solution, while part of remaining actinide elements were enclosed by glass network. To achieve this aim, compact microstructure was obligatory and important for generated glass-ceramics, which required uniform grain size and uniform distribution of crystalline phase in glass phase. Three stages were experienced for specimen with set material components and sintering temperature along the sintering process, which were, respectively, shrinkage accelerating stage, shrinkage retarding stage, and shrinkage stagnating stage.

The bulk density variations of specimens obtained at different sintering temperatures and holding time were, respectively, illustrated in Figs. 3 and 4. As shown in Fig. 3, the bulk density of specimen firstly increased quickly with the rising of sintering temperature until 930 °C, then gradually decreased with further rising of sintering temperature ( $\geq 940$  °C), indicating that crystallization temperature of specimen was lower than 940 °C. The formation of crystal hindered the movement of particles inside specimen and thus hindered further sintering and densification for specimen. As to the relationship between the bulk density and holding time, as shown in Fig. 4, the bulk density in general raised with holding time. The bulk density increased quickly when holding time was raised from 0.5 h to 1.5 h, while the rise in bulk density was largely mitigated as holding time was further increased (2–3 h) and was fairly smooth over time (3.5–4 h).

**Fig. 3** Bulk density of specimen changes with sintering temperature

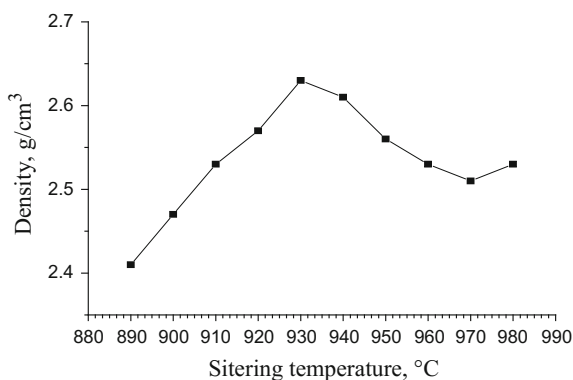


**Fig. 4** Bulk density of specimen changes with holding time

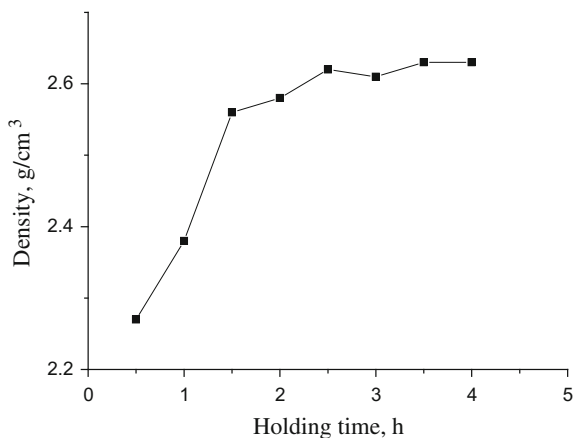


**Table 5** PCT results after 7 days of soaking

| Sample | Leaching rate ( $\times 10^{-4}$ )/g m <sup>-2</sup> d <sup>-1</sup> |        |      |
|--------|--|--------|------|
|        | Fe   | P      | Ce   |
| A      | 11.04  | 44.43  | 1.13 |
| B      | 28.10  | 56.61  | 0.95 |
| C      | 77.75  | 85.56  | 0.69 |
| D      | 110.80   | 151.36 | 0.62 |

#### 1.2.4 Pack Capacity for Simulated Wastes and Chemical Durability

The crystal phase change in the glass-ceramic solidified body together with the leaching rate of key elements was investigated when pack capacity for simulated wastes in solidified body was, respectively, 20, 25, 30, and 35 %. All the glass-ceramic solidified bodies were prepared with optimized process parameters, and relative results were summarized in Fig. 3 and Table 5.

Figure 5 shows the XRD patterns of part specimens. As shown, when pack capacity for simulated wastes in solidified body was 20%, the crystal phase in specimen was basically the single monazite phase; when pack capacity increased to 25%, ferric phosphate patterns began to appear, which was quite distinct as pack capacity further increased to 30%. The mole ratio of Fe to P in solidification matrix increased with the pack capacity for simulated wastes, which changed the structure of iron boron phosphate basic glass. The chemical durability of basic glass was weakened, and the main crystal phase in solidification matrix changes from single monazite phase to co-existent phase, including monazite and ferric phosphate. The results of normalized leaching rate of key elements (Table 5) also demonstrated that chemical durability of basic glass would be weakened with its rising pack capacity for simulated wastes since elemental mass release of Fe and P gradually increased. However, the content of element Ce in simulated wastes was still within the largest

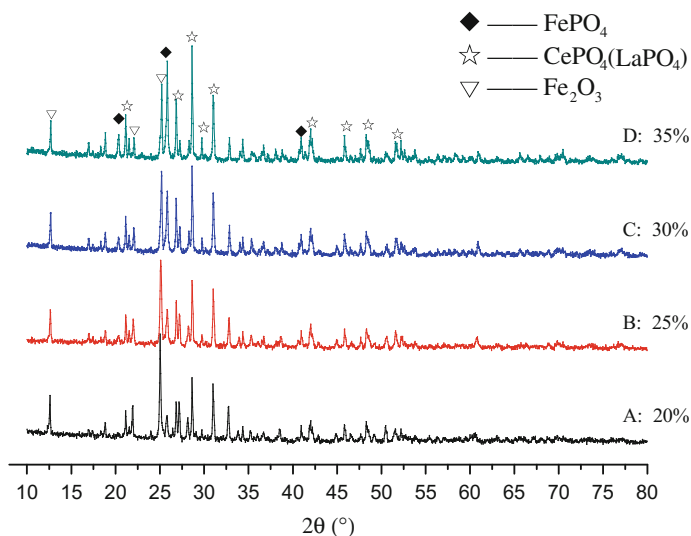


**Fig. 5** XRD patterns of part specimens

pack capacity of such glass system [6], which could firmly “imprison” Ce and keep its leaching rate almost stable at  $10^{-5}$ . Hence, the pack capacity for simulated wastes should be no more than 25% in order to obtain glass-ceramic solidification matrix of good performance.

## 2 Website

### 2.1 Website of PBNC2016

The website of PBNC2016 is <http://www.pbnc2016.org/>. For more information, please visit the website.

## 3 Conclusions

In this study, the simulated high-level radioactive wastewater generated from TRPO extraction process was solidified using iron boron phosphate glass, and its solidification parameters including sintering temperature, holding time, and waste pack capacity were investigated. Glass-ceramic solidification matrix with monazite as main crystal phase could be obtained at sintering temperature of 930 °C holding for 2 h. Elements La and Ce in simulated wastes were steadily enclosed in monazite

phase by solidification matrix. The recommended maximum pack capacity for simulated wastes was 25%. The solidification matrix showed good performance in chemical durability under proposed conditions and normalized leaching rate for simulated actinide element Ce could be kept at  $10^{-5}$ .

**Acknowledgments** This work was supported by “Radiochemistry 909 Program” in China Academy of Engineering Physics (CAEP) and the NSFC (21407133).

## References

1. W. Lutze, R.C. Ewing (Eds). Radioactive waste forms for the future [J]. North-Holland (Amsterdam), 1988:31.
2. Toshinori Okura, Tomoko Miyachi, Hideki Monma. Properties and vibrational spectra of magnesium phosphate glasses for nuclear waste immobilization [J]. Journal of the European Ceramic Society, 2006(26): 831–836.
3. C.P. Kaushik, R.K. Mishra, P. Sengupta, et al. Barium borosilicate glass—a potential matrix for immobilization of sulfate bearing high-level radioactive liquid waste [J]. Journal of Nuclear Materials, 2006, (358): 129–138.
4. Raman K. Mishra, Kumaran V. Sudarsan, Pranesh Sengupta, et al. Role of sulfate in structural modifications of sodium barium borosilicate glasses developed for nuclear waste immobilization [J]. Journal of the American Ceramic Society, 2008, 91(12): 3903–3907.
5. Bingham P A, Yang G, Hand R J, etc. Boron environments and irradiation stability of iron borophosphate glasses analysed by EELS [J]. Solid State Sciences, 2008, 10(9):1194–1199.
6. Liao Qi-long, Wang Fu, Pan She-qi, Liao Hua. Structure and chemical durability of Ce-doped iron borophosphate glasses [J]. Journal of Nuclear and Radiochemistry, 2010, 32(6): 336–341. (in chinese).
7. Song Chong-li. The concept flowsheet of partitioning process for the Chinese high level liquid waste [J]. Atomic Energy Science and Technology, 1995, 29(3): 201–209. (in chinese).
8. M.G. Mesko, D.E. Day, B.C. Bunker. Immobilization of CsCl and SrF<sub>2</sub> in iron phosphate glass [J]. Nuclear and chemical Waste Management, 2000, Volume 20(4):271–278.
9. Cheol-Woon Kim, Delbert E Day, Immobilization of Hanford LAW in iron phosphate glasses, Journal of Non-Crystalline Solids, Volume 331, Issues 1–3, 1 December 2003, Pages 20–31.
10. B.C. SALES, L.A. BOATNER. Lead-Iron Phosphate Glass: A Stable Storage Medium for High-Level Nuclear Waste [J]. Science, 1984, 226(4670):45–48.
11. Pan She-qi, Su Wei. Immobilization of HLLW in iron phosphate glasses [J], Engineering Materials, 2011, 10(4): 76–79. (in chinese).
12. Wang Fu, Liao Qi-long, Pan She-qi, Liao Hua. Effect of Na<sub>2</sub>O on structure and properties of iron borophosphate glasses [J]. Radiation Protection, 2010, 30(4): 208–213. (in chinese).
13. Liao Qi-long, Wang Fu, Pan She-qi, Liao Hua. Structure and chemical durability of Ce-doped iron borophosphate glasses [J]. Journal of Nuclear and Radiochemistry, 2010, 32(6):336–341. (in chinese).
14. Yong He, Y.J. Lü, Q. Zhang, Characterization of monazite glass-ceramics as wasteform for simulated  $\alpha$ -HLLW [J]. J. Nuclear Materials. 376 (2008) 201–206.